*Journal of Oleo Science*
*Copyright ©2024 by Japan Oil Chemists' Society*
*doi : 10.5650/jos.ess24020*
*J. Oleo Sci.* **73**, (10) 1349-1360 (2024)

# *In silico* and *in vitro* Characterizations of Rodent Tuber (*Typhonium flagelliforme*) Mutant Plant Isolates against FXR Receptor on MCF-7 Cells

Nesti Fronika Sianipar[1,2]*, Yuni Elsa Hadisaputri[3,4], Khoirunnisa Assidqi[1,2], Supriatno Salam[5], Muhammad Yusuf[6], Wanda Destiarani[6], Ragapadmi Purnamaningsih[7], Idris Gautama So[8], Kensaku Takara[9,10], and Yonathan Asikin[9,10]

[1] *Biotechnology Department, Faculty of Engineering, Bina Nusantara University, Jakarta 11480, INDONESIA*
[2] *Food Biotechnology Research Center, Bina Nusantara University, Jakarta 11480, INDONESIA*
[3] *Department of Biological Pharmacy, Faculty of Pharmacy, Universitas Padjadjaran, Jatinangor 45363, INDONESIA*
[4] *Biological Activity Division, Central Laboratory, Universitas Padjadjaran, Jatinangor 45363, INDONESIA*
[5] *Faculty of Pharmacy, Universitas Mulawarman, Samarinda 75123, INDONESIA*
[6] *Department of Chemistry, Faculty of Mathematics and Natural Sciences, Universitas Padjadjaran, Jatinangor 45363, INDONESIA*
[7] *Research Center for Horticultural and Estate Crops, National Research and Innovation Agency, Bogor, 16111, INDONESIA*
[8] *Management Department, Binus Business School, Undergraduate Program, Bina Nusantara University, Jakarta 11480, INDONESIA*
[9] *Department of Bioscience and Biotechnology, Faculty of Agriculture, University of the Ryukyus, Nishihara 903-0213, JAPAN*
[10] *The United Graduate School of Agricultural Sciences, Kagoshima University, Kagoshima 890-0065, JAPAN*

**Abstract: *Typhonium flagelliforme* (*T. flagelliforme*) is an Indonesian rodent tuber plant traditionally used to treat cancer diseases. Although gamma-ray irradiation has been used to increase the content in the chemical compounds of the *T. flagelliforme* plants with anticancer activity ten times effective, the specific effect of the isolated compounds from the mutant plants has never been reported yet. The potential cytotoxic agents were characterized via nuclear magnetic resonance spectroscopy, infrared spectroscopy, and mass spectrometry as stigmasterol and 7α-hydroxyl stigmasterol; and their anticancer activity was investigated. The *in silico* biochemical profile of the two compounds were analyzed by molecular docking and molecular dynamics simulation to confirm its interaction with the agonist binding site of Farsenoid X receptor (FXR). Stigmasterol and 7α-hydroxyl stigmasterol can act as a competitive regulator with a high-affinity for the FXR. The results also showed that stigmasterol and 7α-hydroxyl stigmasterol were the most potential and active fraction of the *T. flagelliforme* mutant plant against the MCF-7 human breast cancer cell line, with $IC_{50}$ value 9.13 μM and 12.97 μM, compared with cisplastin as a control about 13.20 μM. These results demonstrate the potential of stigmasterol and 7α-hydroxyl stigmasterol in *T. flagelliforme* mutant plants to act towards cancer diseases.**

**Key words:** *Typhonium flagelliforme*, Farsenoid X receptor, MCF-7 cell line, stigmasterol, mutant plant

## 1 Introduction

*Typhonium flagelliforme* (*T. flagelliforme*) is a rodent tuber herbal plant of the Araceae family from Indonesia. It has demonstrated anticancer activity against various cancer cell lines, including lung and breast cancer cells[1)], T4-lymphoblastoid leukemia[2)], T47D breast cancer[3)], and MCF-7 breast cancer[4)]. By subjecting *T. flagelliforme* plants to gamma-ray irradiation, the content in bioactive compounds can be increased *in vitro* through combined mutagenesis of somaclonal variations. Thus, genetic changes have been detected in *T. flagelliforme* mutants of the first generation (MV1)[5)], and a molecular random amplified polymorphic DNA analysis revealed genetic changes in the second-generation (MV2) and third-generation (MV3) *T. flagelliforme* mutants compared with the wild type[6)]. In 2020, the *T. flagelliforme* mutant plant was included in the Plant Variety Protection list by the Ministry of Agriculture, Republic of Indonesia due to the increasing research interest in its anticancer activity[6–8)]. The ethyl acetate fraction of the superior *T. flagelliforme* mutant is promising as an

*Correspondence to: Nesti Fronika Sianipar, Biotechnology Department, Faculty of Engineering, Bina Nusantara University, 11480 Jakarta, INDONESIA
E-mail: nsianipar@binus.edu
*Accepted July 23, 2024 (received for review January 25, 2024)*
Journal of Oleo Science ISSN 1345-8957 print / ISSN 1347-3352 online
https://www.jstage.jst.go.jp/browse/jos/ https://mc.manuscriptcentral.com/jjocs

CC BY

anticancer agent with an $IC_{50}$ value of 1.09 μg/mL. In contrast, the ethanol extract has an $IC_{50}$ value of 1.60 μg/mL[9], which indicates that the cytotoxic activity of the *T. flagelliforme* mutant extract is ten times higher than that of the wild-type extract.

The concentration of chemical components of the KB 6-3-3-6 *T. flagelliforme* mutant plant extract, which comprised of palmitic acid, octadecadienoic acid, stigmasterol, and beta-sitosterol, obtained by GCMS analysis were higher than in the wild type[10]. Among these compounds, stigmasterol exhibits antioxidant activity against Ehrlich ascites carcinoma (EAC) cells by decreasing lipid peroxidation and increasing the catalase content in the liver of EAC rats[11]. It is the main phytosterol in various herbal plants with anti-inflammatory and anticancer properties[12]. It can inhibit the growth of uterine cancer cells ES2 and OV90 by 50% at a treatment concentration of 20 μg/mL[13]. The extract from *T. flagelliforme* have potential anticancer activity, and the oral nanoemulsion of its extract could be formulated using glycerol, DMSO, tween 80, and water at different concentrations[14]. However, the molecular mechanism of action of stigmasterol isolated from *T. flagelliforme* mutant plants causing MCF-7 breast cancer cell death has not yet been revealed.

*In silico* methods such as molecular docking and dynamics could be used to predict the molecular mechanism of bioactive compounds at the atomic level[15–17]. These methods are critical in designing new drugs because they allow determining the small molecule affinity within the binding site of the desired target receptor. A successful splicing methodology must correctly predict the native ligand to which the receptor binds and the associated physicochemical molecular interactions[18]. However, the active compound from *T. flagelliforme* mutant plants causing MCF-7 breast cancer cell death has not yet been revealed. Therefore, this study aimed to characterize the *in silico* and *in vitro* chemical profiles of *T. flagelliforme* mutant plant isolates against Farsenoid X receptor (FXR) on MCF-7 breast cancer cell line. The active compounds were isolated and identified, and their binding mode and interaction mechanisms with the breast cancer cell line were explored using molecular docking and dynamics simulations, respectively. Additionally, the anticancer activities were clarified using a proliferation assay.

## 2 Experimental Procedures

### 2.1 Plant material

*T. flagelliforme* mutant plant KB 6-3-3-6 was collected from Sianipar and Purnamaningsih's collection from the Indonesian Center for Agricultural Biotechnology and Genetic Resources Research and Development, Ministry of Agriculture, Republic of Indonesia, Bogor, Indonesia. The mutant plants were obtained by irradiating with gamma rays at a dose of 6 Gy to produce mutagenesis *in vitro*. During the acclimation process, the mutant plant KB 6-3-3-6 was maintained at a constant temperature of 28–30℃ and received adequate water to protect the plants against highly susceptible attacks from insects, pathogenic fungi, and bacteria during acclimatization. The KB 6-3-3-6 voucher specimens (reference number TYFL001) have been registered and deposited under plant variety protection rights number 00489/PPVT/S/2020 at the Center for Plant Variety Protection and Agricultural Licensing, Minister of Agriculture, Republic of Indonesia.

### 2.2 Extraction and isolation

The tubers of *T. flagelliforme* mutant KB 6-3-3-6 were harvested at approximately 10.23 kg and dried in room temperature at 25–30℃ to obtain 3.12 kg of tuber powder. The powder was then submerged in ethanol 96% and macerated seven times until the extract was colorless. The solvents were evaporated using a rotary evaporator (Rotavapor R-300, Buchi, Flawil, Switzerland) at 50℃ to obtain a concentrated ethanol extract (143.47 g). A cytotoxic bioguided separation was performed using vacuum liquid chromatography (VLC) with stationary phase of silica gel G60 (70–230 mesh) and mobile phase of hexane:ethyl acetate:methanol (7:2:1 v/v/v, 10% gradient). The resulting fractions were hexane, ethyl acetate (21 fractions), and methanol extracts (7.98, 17.75, and 18.75 g, respectively). Ethyl acetate extract was selected because of the low $IC_{50}$ value of cytotoxic activity against MCF-7 breast cancer cells (see Subsection 2.6). Each ethyl acetate fraction was then analyzed by thin-layer chromatography (TLC) on a 60 GF254 silica plate developed by hexane:ethyl acetate (1:1 v/v) to determine the staining pattern of the compounds. Subfractions were obtained and separated by column chromatography on silica gel G60 (70–230 mesh) using hexane:methylene chloride:ethyl acetate (7:2:1 v/v/v, 5% gradient). The combined subfraction was further collected and separated by column chromatography on silica gel G60 (230–400 mesh) with a solvent system of hexane:methylene chloride:ethyl acetate (6:2.5:1.5 v/v/v, isocratic), from which compounds 1 and 2 were obtained (4.8 and 2.4 mg or 0.003% and 0.0016%, respectively) (Fig. 1).

### 2.3 Spectroscopic characterization of compounds from the mutant plant extract

Infrared spectra in KBr and mass spectrometry (MS) data were recorded on Shimadzu IR Prestige-21 (Shimadzu, Kyoto, Japan) and Waters Xevo QTOF MS (Waters, Milford, USA), respectively. The nuclear magnetic resonance (NMR) spectra were analyzed using JEOL ECZ-500 (JEOL USA, Peabody, USA) and Variant Unity INOVA-500 NMR spectrometers (Agilent Technologies, Santa Carla, USA). The NMR data were recorded at 500 MHz for $^1H$ and 125

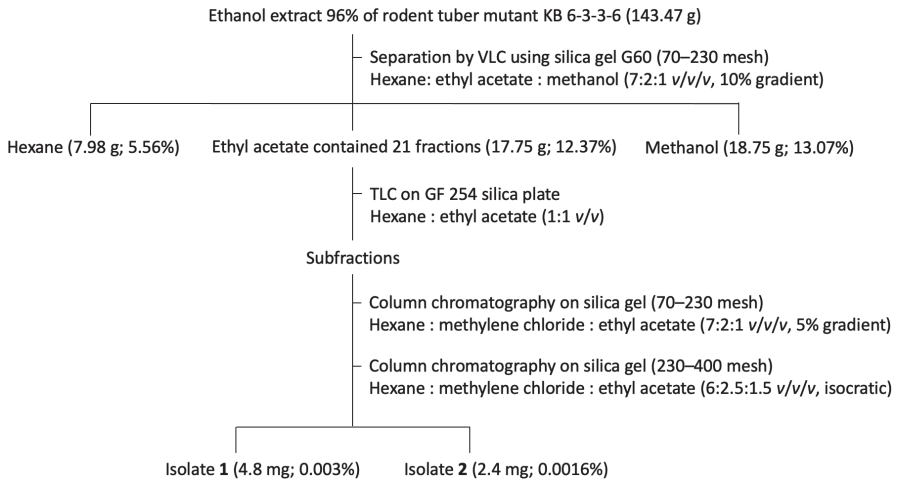



Fig. 1 Isolation scheme for compounds 1 and 2 of *T. flagelliforme* mutant KB 6-3-3-6 extract.

MHz for $^{13}C$ using tetramethylsilane as an internal standard.

### 2.4 *In silico* bioprospection of stigmasterol

The crystal structures of the natural ligand (3-deoxychenodeoxycholic acid; CDCA) and the agonist ligand (tropifexor) binding to the FXR were downloaded from the PDB library (PDB ID: 7D42 and 1OT7)[18, 19]. The structure of the ligands was separated from the receptor using Discovery Studio 2021 (Dassault Systèmes, Vélizy-Villacoublay, France), and the water molecules and heteroatoms were also removed. The three-dimensional (3D) structure of stigmasterol was modeled using Chem3D (University of Bath Library, UK). Docking simulation with a rigid receptor structure was performed with AutoDock 4.2.6 (The Scripps Research Institute, California, USA)[6, 20]. Furthermore, the 3D structure of all the ligands was converted into the PDBQT format by employing the Gasteiger charges and adding the atom types using AutoDock Tools 1.5.6 (The Scripps Research Institute). The size of the grid box of the receptor, centered on the ligand's binding site, was 40 × 40 × 50 points with a grid spacing of 0.375 Å. The Lamarckian Genetic algorithm was used with the following parameters: trials of 100 runs, energy evaluations of 2,500,000, and population size of 150. The energy breakdown and ligand efficiency (total binding energy divided by the number of atoms) were also calculated. The docking result was visualized using Biovia Discovery Studio Visualizer (Dassault Systèmes) and sorted based on the free energy of the binding on the most populated cluster and their intermolecular interactions.

### 2.5 Molecular dynamics simulation

In this study, four simulation systems were prepared using LEaP and antechamber runs of Amber20 (Amber community, San Francisco, USA). The 3D structures of CDCA, tropifexor, and stigmasterol bound to FXR (Chain A of 1OT7) were used as starting structures. The ff14SB, GAFF2, and TIP3P force fields were used. Each of the systems was immersed in TIP3P water box and neutralized by adding $Na^+$ counter ions. The minimization and MD simulations were performed using Amber20. An initial minimization of 1000 steps using the steepest descent algorithm was conducted. Then, 2000 steps of conjugate gradient minimization with 500 kcal/molÅ2 of harmonic restraints were applied to the backbone atoms. Finally, 5000 steps of unrestrained conjugate gradient minimization were performed to remove any steric clashes among the atoms.

The system was gradually heated to the optimum temperature of 37℃, 11 for 60 ps to create an NVT ensemble using harmonic restraints of 5 kcal/molÅ2 on the backbone atoms. Furthermore, 1 ns of NPT equilibration was performed, where harmonic restraints on the backbone were slowly decreased by 1 kcal/molÅ2 until reaching 0.200 ns of the production run in the NPT ensemble was performed with all hydrogen atoms constrained using the SHAKE algorithm. The temperature was controlled with a Langevin thermostat with a collision frequency of 1 $ps^{-1}$, and the pressure was controlled using a Berendsen barostat with a coupling constant of 1 ps and a target pressure of 1 bar. A nonbonded cutoff value of 9 Å was used, and the long-range electrostatics were treated using the particle mesh Ewald method. The MD trajectories were analyzed using the CPPTRAJ module in AmberTools19 (Amber community). Amber and AmberTools are freely available at https://ambermd.org. The binding energy was calculated using the MM-GBSA method in the MMPBSA module.

### 2.6 Cell viability evaluation by PrestoBlue assay

The cell viability of MCF-7 breast cancer cells was evaluated by performing a PrestoBlue assay (Thermo Fisher Scientific, Waltham, USA). MCF-7 cells were purchased from American Type Cell Cancer (Manassas, Virginia, USA) and cultured in Eagle's minimum essential medium containing 10% fetal bovine serum (FBS) and 1% of 100 μg/mL peni-

cillin and 100 μg/mL streptomycin (EMEM, Sigma Aldrich; Darmstadt, Germany). Cisplatin (Sigma Aldrich) was used as a positive control. Each well of a 96-well plate contained the cells to be tested with cultured medium. The test solutions contained 100 μL of medium with stigmasterol from *T. flagelliforme* superior mutant. PrestoBlue solution (100 μL, 10% in medium without FBS) was added to each well plate and incubated at 37℃ and 5% $CO_2$ gas for 24 h. The change in the fluorescence of the test reagent (resazurin to resorufin) was measured using an Infinite M200 PRO microplate reader (Tecan, Männedorf, Switzerland) at excitation wavelengths of 570/600 nm. The conversion value is proportional to the number of metabolically active cells and can be measured quantitatively. The percentage of cell viability equals (absorbance of treated cells/absorbance of untreated cells) × 100%. The $IC_{50}$ value was defined as the amount of concentration that can suppress cancer cell activity by 50% of the initial activity.

## 3 Results

### 3.1 Chemical structure characterization

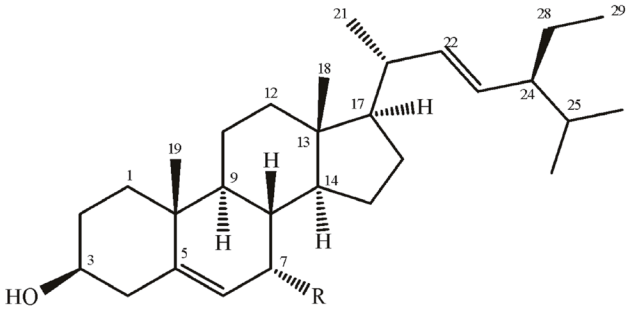
The ethyl acetate fraction obtained from the dry *T. fla-*

Table 1 NMR data of compounds 1 and 2, analyzed at 500 MHz ($^1$H) and 125 MHz ($^{13}$C).

| Carbon position | Compound 1 (stigmasterol) | | Compound 2 (7α-hydroxyl stigmasterol) | |
|---|---|---|---|---|
| | $^1$H-NMR $\delta_{H/ppm}$ (∑H, Mult, J/Hz) | $^{13}$C-NMR $\delta_C$/ppm | $^1$H-NMR $\delta_{H/ppm}$ (∑H, Mult, J/Hz) | $^{13}$C-NMR $\delta_C$/ppm |
| 1 | 1.15, 1.89 (2H, m) | 37.3 | 1.15, 1.86 (2H, m) | 37.3 |
| 2 | 1.85, 1.56 (2H, m) | 31.7 | 1.82, 1.51 (2H, m) | 31.7 |
| 3 | 3.53 (1H, m) | 71.9 | 3.53 (1H, m) | 71.9 |
| 4 | 2.28 (2H, m) | 42.5 | 2.28 (2H, m) | 42.5 |
| 5 | – | 140.9 | – | 140.9 |
| 6 | 5.36 (1H, dd, 2.5, 7.2) | 121.9 | 5.31 (1H, dd, 2.5, 7.2) | 122.0 |
| 7 | 1.53 (2H, m) | 31.9 | 4.42 (1H, dd, 7.5, 6.5) | 73.5 |
| 8 | 1.93 (1H, m) | 31.9 | 1.93 (1H, m) | 32.0 |
| 9 | 0.98 (1H, m) | 50.2 | 0.98 (1H, m) | 50.2 |
| 10 | – | 36.6 | – | 36.6 |
| 11 | 1.51 (2H, m) | 21.2 | 1.51 (2H, m) | 21.2 |
| 12 | 1.19, 2.03 (2H, m) | 39.9 | 1.19, 2.03 (2H, m) | 39.9 |
| 13 | – | 42.4 | – | 42.4 |
| 14 | 1.00 (1H, m) | 56.8 | 1.00 (1H, m) | 55.9 |
| 15 | 1.13, 1.61 (2H, m) | 24.4 | 1.13, 1.61 (2H, m) | 24.4 |
| 16 | 1.35, 1.86 (2H, m) | 28.4 | 1.35, 1.86 (2H, m) | 28.4 |
| 17 | 1.10 (1H, m) | 56.0 | 1.10 (1H, m) | 56.0 |
| 18 | 0.68 (3H, s) | 11.9 | 0.68 (3H, s) | 11.9 |
| 19 | 1.00 (3H, s) | 19.7 | 1.00 (3H, s) | 19.7 |
| 20 | 1.37 (1H, m) | 36.4 | 1.37 (1H, m) | 36.4 |
| 21 | 0.92 (3H, d, 7) | 19.5 | 0.92 (3H, d, 7) | 19.5 |
| 22 | 4.97 (1H, dd, 5.5, 14.2) | 129.4 | 4.97 (1H, dd, 5.5, 14.2) | 129.4 |
| 23 | 5.11 (1H, dd, 2.5, 14.2) | 138.5 | 5.11 (1H, dd, 2.5, 14.2) | 137.9 |
| 24 | 0.97 (1H, m) | 45.9 | 0.97 (1H, m) | 45.9 |
| 25 | 1.70 (1H, m) | 29.2 | 1.70 (1H, m) | 29.2 |
| 26 | 0.84 (3H, d, 7) | 19.0 | 0.84 (3H, d, 7) | 19.1 |
| 27 | 0.82 (3H, d, 7) | 18.9 | 0.82 (3H, d, 7) | 18.9 |
| 28 | 1.27 (2H, m) | 23.2 | 1.27 (2H, m) | 23.2 |
| 29 | 0.85 (3H, t, 7) | 11.9 | 0.85 (3H, t, 7) | 11.8 |

*gelliforme* powder was chromatographed over a vacuum-liquid chromatography (VLC) column, packed with silica gel 60 via gradient elution. The VLC fractions were subjected to preparative thin-layer chromatography (TLC) on silica gel GF254, followed by column chromatography separations to obtain compounds 1 and 2 as a colorless amorphous solid. Its molecular composition was established to be $C_{29}H_{48}O$. According to a high-resolution time-of-flight MS analysis, which showed an $[M+H]^+$ ion peak at *m/z* 413.7744 (calcd. $C_{29}H_{49}O$ *m/z* 413.7714), requiring six degrees of unsaturation. The infrared spectrum showed band at $\nu_{max} = 3495\ cm^{-1}$ ascribable to a hydroxyl group. The $^1$H-NMR spectrum (Table 1) displayed six methyl signals at $\delta_H$ 0.68 (3H, s, H-18), 0.85 (3H, t, H-29), 0.81 (3H, d, H-27), 0.84 (3H, d, H-26), 0.92 (3H, d, H-21) and 1.00 (3H, s, H-19) which is in agreement with the phytosterol group steroid framework. Furthermore, resonances attributable to nine $sp^3$ methylene protons at $\delta_H$ 1.51 (2H, H-11), 1.27 (2H, H-28), 1.13; and 1.61 (2H, H-15), 1.35; and 1.86 (2H, H-16), 1.85; and 1.56 (2H, H-2), 1.53 (2H, H-7), 1.15; and 1.89 (2H, H-1), 1.19; 2.03 (2H, H-12) and 2.28 (2H. H-4) and there are seven methine protons $sp^3$ at $\delta_H$ 1.71 (1H, H-25), 1.91 (1H, H-8), 1.37 (1H, H-20), 0.97 (1H, H-24), 0.98 (1H, H-9), 1.10 (1H, H-17) and 1.00 (1H, H-14), one oxygenated methine proton at $\delta_H$ 3.53 (1H, m, H-3) and three methine protons $sp^2$ at $\delta_H$ 5.36 (1H, dd, 2.5; 7.2 H-6), 4.97 (1H, dd, 5.5; 14.2, H-22) and 5,11 (1H, dd, 4.5; 14.2, H-23) were observed, the latter indicating that the olefinic bond between C-22 and C-23 was a *trans* form (Fig. 2).

The $^{13}$C NMR (Table 1) and DEPT spectra revealed the presence of twenty-nine carbons (Fig. 2), i.e. six methyl carbons at $\delta_C$ 11.9 (C-18), 11.9 (C-29), 18.9 (C-27), 19.0 (C-26), 19.5 (C-21), and 19.7 (C-19), nine methylene carbon $sp^3$ at $\delta_C$ 21.2 (C-11), 23.2 (C-28), 24.4 (C-15), 28.4 (C-16), 31.7 (C-2), 31.9 (C-7), 37.3 (C-1), 39.9 (C-12) and 42.5 (C-4) and there are seven methine carbons $sp^3$ at $\delta_C$ 29.2 (C-25), 31.9 (C-8), 36.4 (C-20), 45.9 (C-24), 50.2 (C-9), 56.0 (C-17), 56.8 (C-14), one oxygenated methine carbon at $\delta_C$ 71.9 (C-3), three methine carbons $sp^2$ at $\delta_C$ 121.9 (C-6), 129.4 (C-22) and 138.5 (C-23), two quaternary carbon $sp^3$ at $\delta_C$ 36.6 (C-10), 42.4 (C-13) and one quaternary carbon at $\delta_C$ 140.9 (C-5). The planar structure was deduced using $^1$H-$^1$H-COSY and HMBC spectra analysis, and the carbon arrangement was observed as stigmasterol[21]. Furthermore, the only hydroxyl group was located at C-3, based on the HMBC correlations of H-3 ($\delta_H$ 3.53) to C-1 ($\delta_C$ 37.3), C-4 ($\delta_C$ 41.5) and C-5 ($\delta_C$ 140.9); H-1 ($\delta_H$ 1.15 and 1.89) to C-3 ($\delta_C$ 71.9). Taken together, the spectroscopic results allowed identifying compound 1 as stigmasterol and compound 2 as 7α-hydroxyl stigmasterol.




1. R= H
2. R= OH

Fig. 2 Structures of compounds (1-2), isolated *T. flagelliforme* mutant plant.

7α-Hydroxyl stigmasterol (2) was found to be a colorless amorphous solid with a molecular composition of $C_{29}H_{48}O_2$ based on HR-TOFMS. This solid showed a molecular ion ($[M+H]^+$) peak at *m/z* = 429.3654 (calculated $C_{29}H_{49}O_2$ *m/z* = 429.3650), which required six degrees of unsaturation. Its infrared spectrum showed bands that were ascribed to a hydroxyl group ($\nu_{max} = 3489\ cm^{-1}$). Its NMR data summarized in Table 1 resembled 1, except the absence of a methylene proton and the presence of an oxygenated proton ($\delta_H$ 4.42 (1H, dd, H-7); $\delta_C$ 73.5 (C-7)). The data suggested that 2 was likely the 7-hydroxyl derivative of 1. This assignment was supported by the HMBC correlation of $\delta_H$ 4.42 (H-7) with $\delta_C$ 140.9 (C-5), 121.9 (C-6), 50.2 (C-9) and 56.8 (C-14). The observed key NOESY correlations between the protons H-7 and H-8 and $CH_3$-19 suggested an α-orientation of the hydroxyl group at C-7.

### 3.2 FXR- stigmasterol docking

The binding mode of stigmasterol in the FXR was investigated from its crystal structure (PDB ID: 7D42). It showed that the interactions between stigmasterol and FXR are favorable and tend to be stable. The ligand-binding site was in the center of FXR-ligand binding domain (LBD), which is around the helix-3, helix-5, helix-6, and helix-10 (Fig. 3a). It is also far from the NcoA co-regulator peptide binding site. Hence it can be assumed that there will be no alteration in the whole structure conformation of FXR-LBD. The lowest binding energy of stigmasterol-FXR is −12.02 kcal/mol and the 7α-hydroxyl stigmasterol is −11.86 kcal/mol. As for the tropifexor as an established drug is −13.15 kcal/mol while the binding with 3-deoxy CDCA as its natural ligand results in −11.17 kcal/mol (Table 2). The average RMSD value of stigmasterol and 7α-hydroxyl stigmasterol conformations are lower than 2 Å (Figs. 3b, 3c) which also proved the stability of its binding with FXR. However, the 7α-hydroxyl stigmasterol presented more alteration in each torsion.

It is shown that the hydroxyl groups in the C2 atom of both stigmasterol formed hydrogen bonds with Thr288. The steroidal core of stigmasterol and 7α-hydroxyl stigmasterol formed a CH-π interaction with Trp454, Leu287, and Ala291. The rest of the interactions between stigmasterol and FXR were hydrophobic (Fig. 4). The other hy-

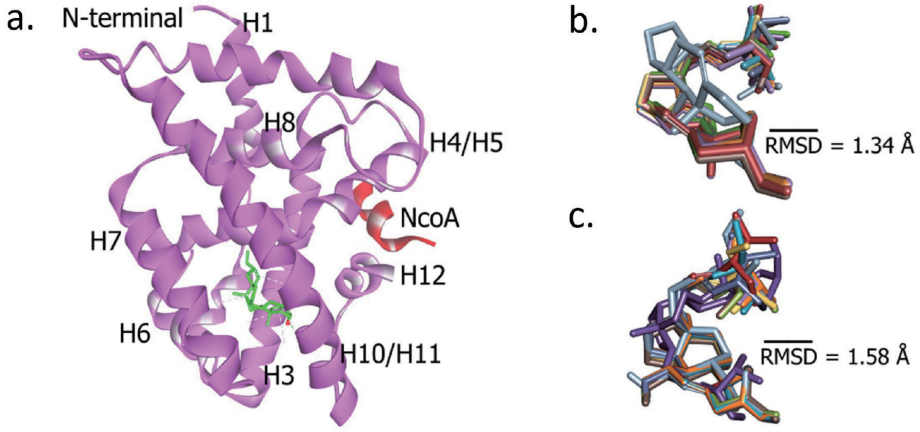



Fig. 3 3-D docking pose of stigmasterol-FXR complex: (a) The LBD of FXR, stigmasterol, and NcoA co-regulator peptide are shown in magenta, green, and red colors, respectively. The calculator RMSD values and average conformations of stigmasterol and 7α-hydroxyl stigmasterol during molecular docking are shown in (b) and (c), respectively. The color differences represent average docking poses in 100 runs.

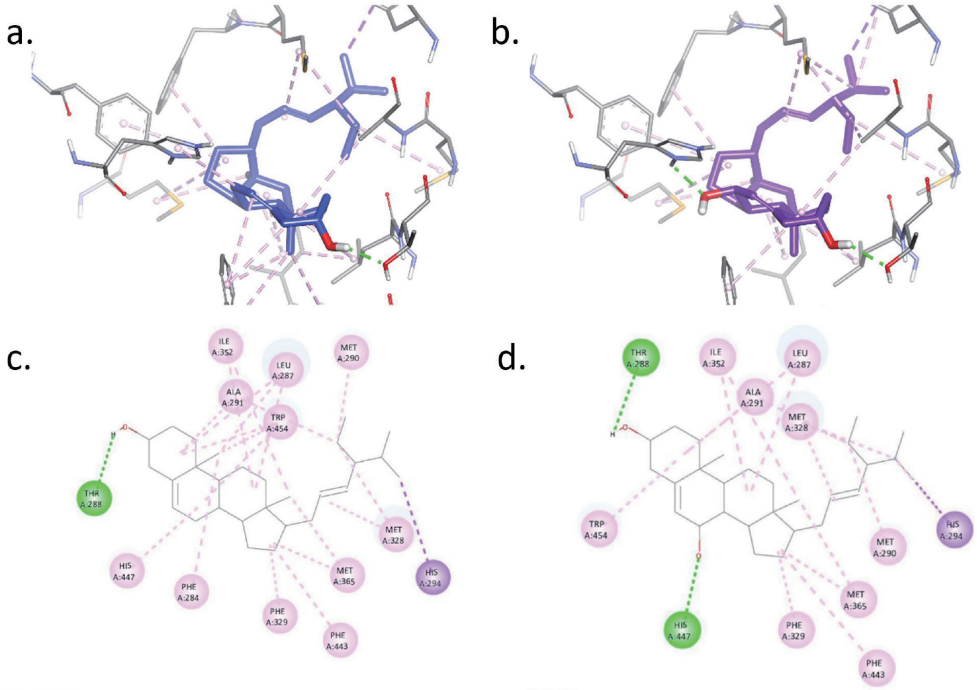



Fig. 4 Ligand-receptor interactions between stigmasterol and FXR: (a) stigmasterol and (b) 7α-hydroxyl stigmasterol as steroid ligands. The 2-dimensional visualization of (c) stigmasterol and (d) 7α-hydroxyl stigmasterol-FXR interactions. Green and white-purple colors represent the hydrogen bon and hydrophobic interactions.

droxyl group in 7α-hydroxyl stigmasterol also promotes hydrogen bonds. Overall, it can be assumed that hydrophobic interactions play a significant role in binding stability. In this work, the results from a PrestoBlue assay showed that stigmasterol and 7α-hydroxyl stigmasterol could inhibit the activity of the MCF-7 cell line, which is consistent with the above findings. As displayed in Figs. 3 and 4 both stigmasterol compounds could be docked to FXR, resulting in a high binding affinity caused by hydrophobic interactions. It is indicated that the steroid moiety in the structure of stigmasterol and 7α-hydroxyl stigmasterol might be crucial for the binding affinity.

### 3.3 Simulation of the FXR stigmasterol interactions

The overall structural stability of FXR in all systems (stigmasterol, CDCA, and tropifexor) was evaluated by RMSD (Fig. 5a). The stigmasterol system was generally the most stable in terms of the FXR conformation (average

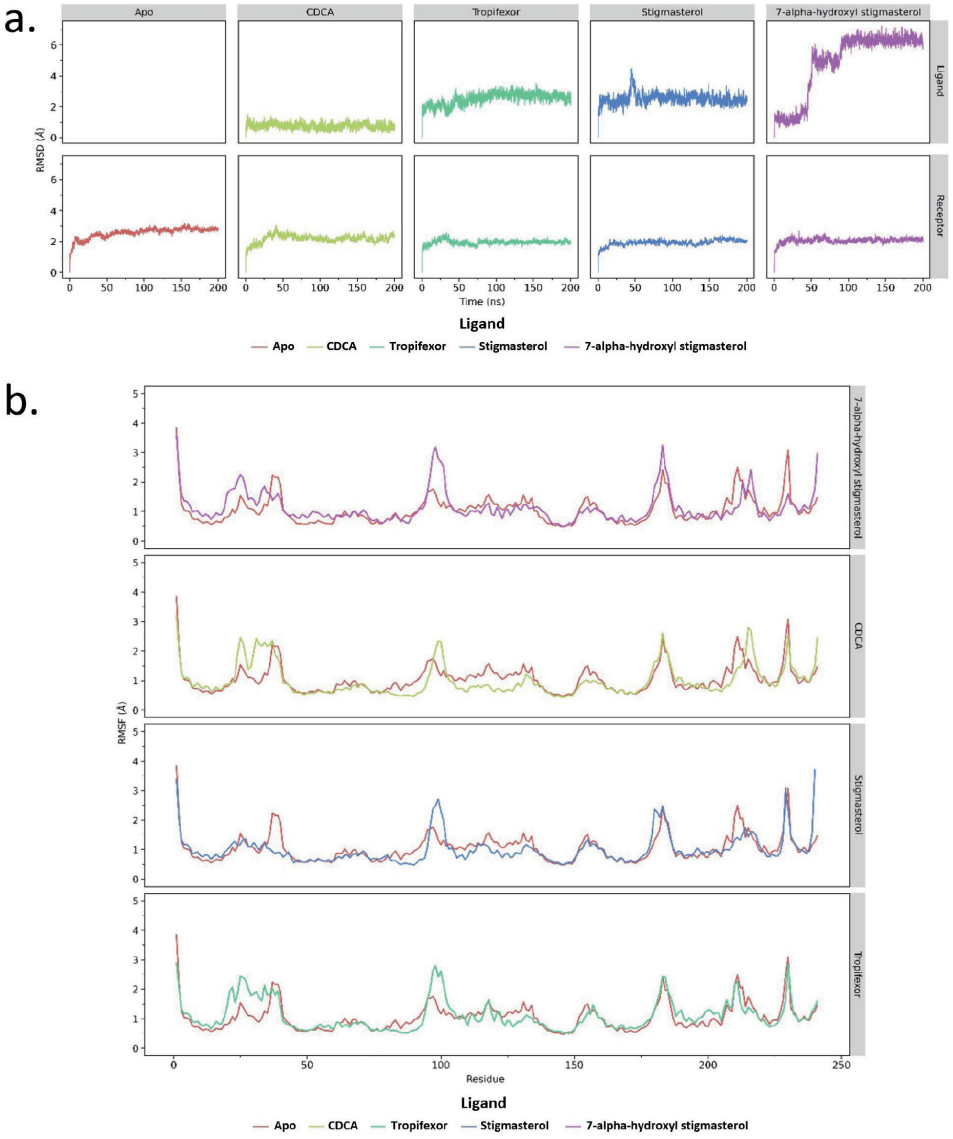



Fig. 5 (a) RMSD of the FXR backbone and the ligand and (b) RMSF of each residue of FXR in all four molecular dynamics systems throughout 200 ns of simulation.

value of 2.43 Å). As for 7α-hydroxyl stigmasterol, the RMSD value fluctuates about three times and becomes stable in the last 100 ns. This fluctuation can present the conformation's changes throughout the simulation. Based on the ligand's RMSD value, the interaction of FXR receptor and CDCA as its natural ligand was quite stable with ΔG° MMGBSA value of −75.51 kcal/mol (Table 2). Furthermore, the residual fluctuation of all systems was computed by the root-mean-square fluctuation calculation (Fig. 5b). The highest fluctuations were observed in the N-terminal and C-terminal because these regions were not restrained, whereas the fluctuation of the binding site (around residue numbers 25−50, and 110−135) in all ligand's systems was also high. Other high fluctuations were observed around residues 180, 210, and 230 due to the natural flexibility of the loop structure. The overall of both stigmasterol systems profile was relatively similar to CDCA and tropifexor in terms of the RMSF parameter and the ΔG° MMGBSA value which was −67.90 kcal/mol for stigmasterol, and −68.89 kcal/mol for tropifexor (Table 2). However, 7α-hydroxyl stigmasterol showed less affinity towards FXR receptor with −55.08 kcal/mol. This indicates that stigmasterol might act as a competitive activator with a single high-affinity binding site on FXR.

The molecular absorption, distribution, metabolism, and toxicity profiles of the stigmasterol compounds in ADMET prediction models are shown in Table 3. The molecular approach of ADMET analysis was carried out using the PreADMET program to explore the properties of both stigmasterol compounds[19, 20]. The results showed that all ligands

Table 2 The binding affinity energy of ligands on FXR system.

| Ligand | Binding energy (kcal/mol) | ΔG° MMGBSA (kcal/mol) | Description |
|---|---|---|---|
| CDCA | −11.17 | −75.51 | Natural ligand |
| Tropifexor | −13.15 | −68.89 | Agonist ligand (established drug) |
| Compound 1 (stigmasterol) | −12.02 | −67.90 | Isolated from *T. flagelliforme* mutant plant |
| Compound 2 (7α-hydroxyl stigmasterol) | −11.86 | −55.08 | Isolated from *T. flagelliforme* mutant plant |

Table 3 The ADMET analysis of ligands using PreADMET server.

| Ligand | Absorption | | Distribution | | Metabolism | | | | Toxicity | |
|---|---|---|---|---|---|---|---|---|---|---|
| | HIA (%) | Caco2 (nm/s) | PPB (%) | BBB (Cbrain / Cblood) | CYP2C19 | CYP2C9 | CYP2D6 | CYP3A4 | Mutagenicity | Carcinogenicity (Mouse/Rat) |
| CDCA | 92.97 | 20.90 | 100.00 | 1.29 | No | Yes | No | Yes | Non | (–) / (+) |
| Tropifexor | 100.00 | 38.33 | 94.21 | 1.18 | No | Yes | No | Yes | Non | (–) / (–) |
| Compound 1 (stigmasterol) | 100.00 | 52.34 | 100.00 | 19.89 | No | Yes | No | Yes | Non | (+) / (–) |
| Compound 2 (7α-hydroxyl stigmasterol) | 94.43 | 36.64 | 100.00 | 14.31 | No | Yes | No | Yes | Non | (+) / (–) |

were well absorbed in the intestine, as indicated by their high HIA percentages, wherein tropifexor and stigmasterol got the maximum scores, and the other compounds also scored no less than 90%. Moreover, stigmasterol had the highest Caco2 permeability ability than the other ligands (52.34 vs. <20 nm/s, respectively). All ligands had high PPB distribution percentages, suggesting that they could be highly soluble in blood and well-dispersed throughout the body, and thus having good stability in the bloodstream and good half-life. The BBB ($C_{brain}/C_{blood}$) value also showed that both stigmasterol compounds have high chances to cross the brain barrier with the ratio of 19.89 and 14.31, compared to tropifexor and CDCA which only had BBB ratio less than 2. On the other hand, all ligands were suitable substrates for two of four cytochrome P450 enzymes, i.e., CYP2C9 and CYP3A4, showing their potent involvement in the metabolism of a wide range of drugs. Candidate compounds, serving as substrates, may either induce CYP enzymes, boosting their activity and enhancing the metabolism of other CYP substrates, or act as inhibitors, suppressing CYP enzyme activity, thereby reducing the metabolism of other drugs and increasing exposure to the candidate compound. Additionally, the mutagenicity and carcinogenicity traits showed all ligands as non-mutagenic candidates, and thus unlikely to induce cancer diseases on mice or rats.

### 3.4 Cytotoxicity of stigmasterol on MCF-7 cell line

The inhibition activity of the *T. flagelliforme* mutant plant isolates identified as stigmasterol and 7α-hydroxyl stigmasterol against the MCF-7 breast cancer cell line was evaluated for 24 h. The minimum concentration of the extract giving a 50% inhibition ($IC_{50}$) in stigmasterol and 7α-hydroxyl stigmasterol were about 9.13 μM and 12.97 μM, respectively (Table 4). As a positive control, cisplatin had $IC_{50}$ value of 13.20 μM against to MCF-7 cancer cell line. According to the criteria of the National Cancer Institute, crude extracts with $IC_{50} \leq 20$ μg/mL has high cytotoxic; between 21 and 200 μg/mL has moderate cytotoxic; between 201 and 500 μg/mL has weak cytotoxic; and $IC_{50} >$ 501 μg/mL has no cytotoxicity effects[22]. Hence, the $IC_{50}$ values of both stigmasterols demonstrated its robust cytotoxic activity against the MCF-7 cell line. After treatment with both stigmasterols for 24 h, slow cell proliferation was observed. Therefore, both stigmasterols have greater cytotoxicity potentials against MCF-7 breast cancer cell lines than cisplatin. This significant anticancer effect suggests that the bioactivity of the *T. flagelliforme* mutant plant might be attributable to stigmasterol compounds. This study indicates that the stigmasterols isolated from *T. fla-*

Table 4 $IC_{50}$ value cytotoxic activity of isolated compounds from *T. flagelliforme* mutant plant against MCF-7 breast cancer cell line.

| Compound | $IC_{50}$ (μM) |
|---|---|
| Compound 1 (stigmasterol) | 9.13 |
| Compound 2 (7α-hydroxyl stigmasterol) | 12.97 |
| Positive control (cisplatin) | 13.20 |

Cells were incubated with various concentrations of isolated compounds for 24 h. The $IC_{50}$ value represents the concentration causing 50% growth inhibition. Data are expressed as means ± SD of three replicates.

*gelliforme* mutant have more potential in inhibiting the cell proliferation of MCF-7 cell lines than the crude and other fraction extracts.

## 4 Discussion

Stigmasterol has been investigated for its pharmacological activities, such as antiosteoarthritic, antihypercholesterolemic, cytotoxicity, antitumor, hypoglycemic, antimutagenic, antioxidant, anti-inflammatory, and CNS effects[23]. The anticancer potential of stigmasterol on various cancer types has been revealed recently. For example, in lung cancer, it reduces Bcl-2 expression as an antiapoptotic protein and enhances the activity of BAX as a proapoptotic protein[24]. The development of skin cancer can also be suppressed by VEGFR-2 and TNF-α downregulation[25], lipid peroxide enhancement, and by causing DNA damage[26]. The stigmasterol also induces the expression of p53 protein while inhibiting the expression of p21 and p27 protein to repress prostate cancer development[27]. Furthermore, stigmasterol induces growth inhibition and apoptosis *in vitro* in a time-dependent and dose-dependent manner[28].

Stigmasterol is the major compound in several plant extracts, including the Chinese medicinal herb *Ophiopogon japonicas* (Maidong in Chinese)[29], leaf extract of *Annona muricata*[30], stem bark of *Neocarya macrophylla*[31], and root extracts from India *Pluchea indica*[32]. In fact, compound 1, stigmasterol, proved to be more active than cisplatin, exhibiting an $IC_{50}$ value of 13.2 μM[33]. Li *et al.*[34] reported that stigmasterol inhibits the proliferation and induces cell apoptosis in human gastric cancer cell line SNU-1 through JAK/STAT signaling pathway with an $IC_{50}$ value of 15 μM. It has been clarified that stigmasterol can induce apoptosis and autophagy in gastric cancer cells by blocking the Akt/mTOR signaling pathway[35]. Stigmasterol isolated from an *n*-hexane extract of *Cheilanthes tenuifolia* has an $IC_{50}$ value of about 205.984 μg/mL on shrimp nauplii, and that isolated from *Bacopa monnieri* inhibited tumor cells of EAC-bearing mice of 60.11% at 10 mg/kg[11]. Al-Fatlawi[36] reported that stigmasterol exerts antiproliferative activity against the human cancerous breast MCF-7 cancer line with an $IC_{50}$ value of about 27.38 μM. Meanwhile, the $IC_{50}$ cytotoxicity concentration of stigmasterol was obtained from *Kopsia singapurensis* Ridl. against the MCF-7 cell line was 14.5 μg/mL[37].

In another study, the stigmasterol isolated from *Polygonum hydropiper* L. was more effective against MCF-7 at 1 mg/mL concentration, killing 87.50% cancerous cells[38]. Our result regarding the cytotoxic activity of stigmasterol against MCF-7 cells is consistent with the previous works. However, the $IC_{50}$ value of the stigmasterol isolated from the *T. flagelliforme* mutant plant is much lower than that of the stigmasterol obtained from other plants. The plant extracts exhibiting an $IC_{50} \leq 4$ μg/mL are considered the most effective cytotoxic agents against cancerous cells, outperforming the crude extracts and pure compounds[39]. The $IC_{50}$ value of the stigmasterol isolated from the *T. flagelliforme* mutant plant is 9.13 μM, which is much lower than that of the extract with a concentration of 1.60 μg/mL and the ethyl acetate fraction with 1.09 μg/mL[9]. Our previous studies demonstrated that triterpenoids (pentandrucines A to K) isolated from the *n*-hexane extract of *Chisocheton pentandrus* exhibit a more robust cytotoxic activity against MCF-7 breast cancer cells *in vitro* with an $IC_{50}$ value of 16.84 μM than the crude extract[40]. According to Tasyriq *et al.*[41] clearly indicated the potential benefits of phytosterol oxides, specifically 7α-hydroxy-β-sitosterol in the prevention of breast adenocarcinoma. Current cytotoxicity data have demonstrated that $IC_{50}$ values of CT1 after 24 h of incubation on all cancer cell lines tested were within the range of 16.0 μM to 32.0 μM, which is comparable to most commercialized phytocompounds[41].

FXR is a member of the nuclear receptor superfamily, which regulates bile acid homeostasis. A high level of FXR expression has been detected in epithelial cells of normal- and tumor breast-cells and invasive ductal carcinoma cells. FXR was also found in human breast cancer cells (MCF-7) and carcinoma cells (MDA-MB-468)[42]. Moreover, in the MCF-7 cell line, FXR activation has been found to downregulate breast cancer target genes (e.g., MRP-1, MDR3, SLC7A5, and aromatase) with the cell proliferation inhibition[14, 16]. Several research groups have also shown that stigmasterol is a potent FXR agonist in breast cancer[43–46]. ADMET *in silico* properties revealed high permeability for human intestinal stigmasterol and the blood–brain barrier; moreover, high target protein binding stability (*in vitro* and *in vivo*) showed low toxicity of this phytosterol[47, 48]. In the metabolism aspect, the commercial drug tropifexor, CDCA, and both stigmasterol compounds were found to be suitable substrates for 2 of 4 types of CYP enzymes. It has been assumed that the clearance of these ligands was independent on the CYP enzyme[49]. The toxic properties are critical in drug design and development; however, the data for the commercial and commonly used drug suggested that the cancer risk prediction was not always implemented[40, 50]. Nevertheless, all the ligands are favorably non-mutagenic. The results confirmed the proper drug-like characteristics and potency cytotoxicity of stigmasterol and 7α-hydroxyl stigmasterol against the *T. flagelliforme* mutant plant.

## 5 Conclusion

In summary, the potential anticancer activity of stigmasterol isolated from the *T. flagelliforme* mutant plant against MCF-7 breast cancer cell line *in vitro* with an $IC_{50}$

value of 9.13 μM has been demonstrated. Stigmasterol can induce oxidative stress in the MCF-7 cells, leading to apoptosis by acting as a competitive activator with a single high-affinity binding site on FXR via hydrophobic interactions. The molecular docking study and MD simulations showed that the interactions stigmasterol and 7α-hydroxyl stigmasterol with FXR are favorable, and its binding energy is to that of the established drug tropifexor and its natural ligand. The results suggest that the cytotoxic effect of stigmasterol toward MCF-7 cells may be due to the strong interaction with the agonist binding site of the FXR receptor which can present as a new insight in breast cancer mechanism.

## Acknowledgment

This research was supported by Bina Nusantara University through a lecturer research grant with No. Contract: 014/VR.RTT/II/2020.

## Conflict Interest

The authors declare no conflicts of interest.

## References

1) Lai, C.S.; Mas, R.H.M.H.; Nair, N.K.; Mansor, S.M.; Navaratnam, V. Chemical constituents and *in vitro* anticancer activity of *Typhonium flagelliforme* (Araceae). *J. Ethnopharmacol.* **127**, 486-494 (2010).
2) Mohan, S.; Abdul, A.B.; Abdelwahab, S.I.; Al-Zubairi, A.S.; Sukari, M.A. *et al. Typhonium flagelliforme* ihibits the proliferation of murine Leukemia WEHI-3 cells *in vitro* and induces apoptosis *in vivo*. *Leuk. Res.* **34**, 1483-1492 (2013).
3) Nurrochmad, A.; Lukitaningsih, E.; Meiyanto, E. Anti cancer activity of rodent tuber (*Typhonium flagelliforme* (Lodd.) blume on human breast cancer T47D cells. *Int. J. Phytomedicine* **3**, 138-146 (2011).
4) Putra, A.; Tjahyono; Winarto. The effectiveness of *Typhonium flagelliforme* tuber extract of diclorometanolic fraction on the inhibition of proliferation of MCF-7 human breast cancer cell-line. *J. Indones. Med. Assoc.* **62**, 5-10 (2012).
5) Sianipar, N.F.; Purnamaningsih, R.; Gumanti, D.L.; Rosaria; Vidianty, M. Analysis of gamma irradiated fourth generation mutant of rodent tuber (*Typhonium flagelliforme* Lodd.) Based on morphology and RAPD markers. *J. Teknol.* **78** (5-6), 41-49 (2016).
6) Sianipar, N.F.; Purnamaningsih, R.; Gumanti, D.L.; Rosaria; Vidianty, M. Analysis of gamma irradiated-third generation mutants of rodent tuber (*Typhonium flagelliforme* Lodd.) Based on morphology, RAPD, and GC-MS markers. *Pertanika J. Trop. Agric. Sci.* **40**, 185-202 (2017).
7) Sianipar, N.F.; Purnamaningsih, R.; Darwati, I.; Laurent, D. Gas Chromatography-Mass Spectrometry (GC-MS) analysis of phytochemicals of first generation gamma-irradiated *Typhonium flagelliforme* Lodd. mutants. *J. Teknol.* **78** (10-4), 1-7 (2016).
8) Sianipar, N.F.; Assidqi, K.; Purnamaningsih, R.; Herlina, T. *In vitro* cytotoxic activity of rodent tuber mutant plant (*Typhonium flagelliforme* Lodd.) against to MCF-7 breast cancer cell line. *Asian J. Pharm. Clin. Res.* **12**, 185-189 (2019).
9) Sianipar, N.F.; Hadisaputri, Y.E.; Assidqi, K.; Simanjuntak, P.; Purnamaningsih, R. A study of anticancer activity from the fractions of rodent tuber superior mutant extract (*Typhonium flagelliforme*) by Prestoblue assay method. *Rasayan J. Chem.* **13**, 1992-1998 (2020).
10) Sianipar, N.F.; Purnamaningsih, R. Enhancement of the contents of anticancer bioactive compounds in mutant clones of rodent tuber (*Typhonium flagelliforme* Lodd.) based on GC-MS analysis. *Pertanika J. Trop. Agric. Sci.* **41**, 305-320 (2018).
11) Ghosh, T.; Maity, T.K.; Singh, J. Evaluation of antitumor activity of stigmasterol, A constituent isolated from *Bacopa monnieri* Linn aerial parts against Ehrlich ascites carcinoma in mice. *Orient. Pharm. Exp. Med.* **11**, 41-49 (2011).
12) Kangsamaksin, T.; Chaithongyot, S.; Wootthichairangsan, C.; Hanchaina, R.; Tangshewinsirikul, C.; Svasti, J. Lupeol and stigmasterol suppress tumor angiogenesis and inhibit Cholangiocarcinoma growth in mice via downregulation of tumor necrosis factor-A. *Plos One* **12**, e0189628 (2017).
13) Sianipar, N.F.; Yuliani, S.; Purnamaningsih, R.; Assidqi, K.; Abbas, B.S. The physical and chemical analysis of nanoemulsion from extract rodent tuber mutant plant (*Typhonium flagelliforme* Lodd.). *IOP Conf. Ser. Earth Environ. Sci.* **439**, 012005 (2020).
14) Bae, H.; Song, G.; Lim, W. Stigmasterol causes ovarian cancer cell apoptosis by inducing endoplasmic reticulum and mitochondrial dysfunction. *Pharmaceutics* **12**, 488 (2020).
15) Mohamad, R.M.N.; Mohd, A.S.; Abu Bakar, M.H.; Razali, S.A.; Mohamed, Z.R.; Ya'akob, H. Molecular docking studies of bioactive compounds from *Annona muricata* Linn as potential inhibitors for BCL-2, BCL-W and MCL-1 antiapoptotic proteins. *Apoptosis* **23**, 27-40 (2018).
16) Biswal, R.A.; Venkataraghavan, R.; Pazhamalai, V.; Romauld, S.I. Molecular docking of various bioactive compounds from essential oil of *Trachyaspermum*

*ammi* against the fungal enzyme Candidapepsin-1. *J Appl Pharm Sci.* **9**(5), 21-32(2019).
17) George, T.K.; Tomy, A.; Jisha, M.S. Molecular docking study of bioactive compounds of *Withania somnifera* extract against Topoisomerase IV Type B. *Proc. Natl. Acad. Sci. India Sect B - Biol. Sci.* **90**, 381-390 (2020).
18) Guedes, I.A.; De Magalhães, C.S.; Dardenne, L.E. Receptor-ligand molecular docking. *Biophys. Rev.* **6**, 75-87(2014).
19) Jiang, L.; Xiao, D.; Li, Y.; Dai, S.; Qu, L. *et al.* Structural basis of Tropifexor as a potent and selective agonist of Farnesoid X Receptor. *Biochem. Biophys. Res. Commun.* **534**, 1047-1052(2021).
20) Mi, L.Z.; Devarakonda, S.; Harp, J.M.; Han, Q.; Pellicciari, R. *et al.* Structural basis for bile acid binding and activation of the nuclear receptor FXR University ff Virginia Health System. *Mol. Cell* **11**, 1093-1100 (2013).
21) National Center for Biotechnology Information. Pubchem Compound Summary for CID 5280794, Stigmasterol. Retrieved January 9, 2024 from https://Pubchem.Ncbi.Nlm.Nih.Gov/Compound/Stigmasterol (2024).
22) Yin, R.; Li, T.; Tian, J.X.; Xi, P.; Liu, R.H. Ursolic acid, a potential anticancer compound for breast cancer therapy. *Crit. Rev. Food Sci. Nutr.* **58**, 568-574(2017).
23) Bakrim, S.; Benkhaira, N.; Bourais, I.; Benali, T.; Lee, L.H. *et al.* Health benefits and pharmacological properties of stigmasterol. *Antioxidants* **11**, 1-32(2022).
24) Qian, S.; Wei, Z.; Yang, W.; Huang, J.; Yang, Y.; Wang, J. The role of BCL-2 family proteins in regulating apoptosis and cancer therapy. *Front. Oncol.* **12**, 1-16 (2022).
25) Parveen, A.; Subedi, L.; Kim, H.W.; Khan, Z.; Zahra, Z. *et al.* Phytochemicals targeting VEGF and VEGF-related multifactors as anticancer therapy. *J. Clin. Med.* **8**(350), 1-39(2019).
26) Moon, J.; Kitty, I.; Renata, K.; Qin, S.; Zhao, F.; Kim, W. DNA damage and its role in cancer therapeutics. *Int. J. Mol. Sci.* **24**, 1-19(2023).
27) Singh, S.K.; Banerjee, S.; Acosta, E.P.; Lillard, J.W.; Singh, R. Reveratrol induces cell cycle arrest and apoptosis with docetaxel in prostate cancer cells via A P53/P21$^{waf1/Cip1}$ and P27$^{kip1}$ pathway. *Oncotarget* **8**, 17216-17228(2017).
28) Zhang, X.; Wang, J.; Zhu, L.; Wang, X.; Meng, F. *et al.* Advances in stigmasterol on its anti-tumor effect and mechanism of action. *Front. Oncol.* **12**, 1-13(2022).
29) Chen, M.H.; Chen, X.J.; Wang, M.; Lin, L.G.; Wang, Y.T. *Ophiopogon japonicus* a phytochemical, ethnomedicinal and pharmacological review. *J. Ethnopharmacol.* **181**, 193-213(2016).
30) Ahamed, J.I.; Francy, K.; Priya, A.V.; Prema, K.J.; Steiny, R.P. *et al.* Computational and biological efficacy of stigmasterol against Hela cells and Vero cells-First time isolated from the ethanolic extract of *Annonamuricata* Linn leaves. *J. Mol. Struct.* **1252**, 132186(2022).
31) Mailafiya, M.M.; Yusuf, A.J.; Abdullahi, M.I.; Aleku, G.A.; Ibrahim, I.A. *et al.* Antimicrobial activity of stigmasterol from the atem bark of *Neocarya macrophylla*. *J. Med. Plants Econ. Dev.* **2**, 1-5(2018).
32) Gomes, A.; Saha, A.; Chatterjee, I.; Chakravarty, A.K. Viper and Cobra venom neutralization by sitosterol and stigmasterol isolated from the root extract of *Pluchea indica* Less.(Asteraceae). *Phytomedicine* **14**, 637-643(2007).
33) Dehghan-Nayeri, N.; Darvishi, M.; Mashati, P.; Rezapour-Kalkhoran, M.; Rezaiefard, M.; Younesian, S. Comparison of cytotoxic activity of herbal extracts on the most commonly used breast cancer cell lines (MCF7 and SKBR3): A systematic review. *J. Res. Pharm.* **24**, 1-22(2020).
34) Li, K.; Yuan, D.; Yan, R.; Meng, L.; Zhang, Y.; Zhu, K. Stigmasterol exhibits potent antitumor effects in human gastric cancer cells mediated via inhibition of cell migration, cell cycle arrest, mitochondrial mediated apoptosis and inhibition of JAK/STAT signalling pathway. *J. BUON* **23**, 1420-1425(2018).
35) Zhao, H.; Zhang, X.; Wang, M.; Lin, Y.; Zhou, S. Stigmasterol simultaneously induces apoptosis and protective autophagy by inhibiting Akt/Mtor pathway in gastric cancer cells. *Front. Oncol.* **11**, 1-11(2021).
36) Al-Fatlawi, A.A.Y. Stigmasterol inhibits proliferation of cancer cells via apoptotic regulatory genes. *Biosci. Res.* **16**, 367-374(2019).
37) Shan, L.Y.; Thing, T.C.; Ping, T.S.; Awang, K.; Hashim, N.M. *et al.* Cytotoxic, antibacterial and antioxidant activity of triterpenoids from *Kopsia singapurensis* Ridl. *J. Chem. Pharm. Res.* **6**, 815-822(2014).
38) Ayaz, M.; Sadiq, A.; Wadood, A.; Junaid, M.; Ullah, F.; Zaman, K.N. Cytotoxicity and molecular docking studies on phytosterols isolated from *Polygonum hydropiper* L. *Steroids* **141**, 30-35(2019).
39) Dehghan-Nayeri, N.; Darvishi, M.; Mashati, P.; Rezapor-Kalkhoran, M.; Rezaiefard, M.; Younesian, S. Comparison of cytotoxic activity of herbal extracts on the most commonly used breast cancer cell lines(MCF7 and SKBR3): A systematic review. *J. Res. Pharm.* **24**, 1-22 (2020).
40) Salam, S.; Harneti, D.; Maharani, R.; Nurlelasari; Safari, A. *et al.* Cytotoxic triterpenoids from *Chisocheton pentandrus*. *Phytochemistry* **187**, 1-12(2021).
41) Tasyriq, M.; Najmuldeen, I.A.; In, L.L.A.; Mohamad, K.; Awang, K.; Hasima, N. 7α-Hydroxy-β-sitosterol from *Chisocheton tomentosus* induces apoptosis via dysregulation of cellular Bax/Bcl-2 ratio and cell cycle ar-

rest by downregulating ERK1/2 activation. *Evid. Based Complement. Alternat. Med.* **2012**, 1-12 (2012).
42) Rosdi, M.N.M.; Arif, S.M.; Abu Bakar, M.H.; Razali, S.A.; Zulkifli, R.M.; Ya'akob, H. Molecular docking Studies of bioactive compounds from *Annona muricata* Linn as potential inhibitors for BCL-W and MCL-1 anti-apoptotic protein. *Apopotosis* **23**, 27-40 (2018).
43) Giordano, C.; Catalano, S.; Panza, S.; Vizza, D.; Barone, I. *et al.* Farnesoid X receptor inhibits tamoxifen-resistant MCF-7 breast cancer cell growth through downregulation of HER2 expression. *Oncogene* **30**, 4129-4140 (2011).
44) Journe, F.; Laurent, G.; Chaboteaux, C. *et al.* Farnesol, A Mevalonate Pathway Intermediate, Stimulates MCF-7 Breast Cancer Cell Growth Through Farnesoid-X-Receptor-Mediated Estrogen Receptor Activation. *Breast Cancer Res. Treat.* **107**, 49-61 (2008).
45) Giordano, C.; Barone, I.; Vircillo, V.; Nonclercq, D.; Durbecq, V. *et al.* Activated FXR inhibits leptin signaling and counteracts tumor-promoting activities of cancer-associated fibroblasts in breast malignancy. *Sci. Rep.* **6**, 1-13 (2016).
46) Jiang, L.; Zhang, H.; Xiao, D.; Wei, H.; Chen, Y. Farnesoid X receptor (FXR): Structures and ligands. *Comput. Struct. Biotechnol. J.* **19**, 2148-2159 (2021).
47) Omran, G.; Abd-Alhaseeb, M.; Houssen, M. The anti-tumor effect of stigmasterol on Sorafenib treated human breast cancer cell lines. *Res. Sq*. 1-14 (2021).
48) Salaria, D.; Rolta, R.; Mehta, J.; Awofisayo, O.; Fadare, O.A. *et al.* Phytoconstituents of traditional Himalayan herbs as potential inhibitors of human Papillomavirus (HPV-18) for cervical cancer treatment: An *in silico* approach. *Plos ONE* **17**, e0265420 (2022).
49) Allouche, A.R. Software news and updates Gabedit — A graphical user interface for computational chemistry softwares. *J. Comput. Chem.* **32**, 174-182 (2012).
50) Supriadi, H.; Salam, S.; Abdullah, F.F.; Subarnas, A.; Sidik, R. *et al.* Steroids from the super red dragron fruit (*Hylocereus costaricensis*). *J. Kim.* **13**, 229-233 (2019).

CC BY 4.0 (Attribution 4.0 International). This license allows users to share and adapt an article, even commercially, as long as appropriate credit is given. That is, this license lets others copy, distribute, remix, and build upon the Article, even commercially, provided the original source and Authors are credited.